Updates on the Conceptual Design Study of the Magnets for the Muon Collider Storage Ring

Barbara Caiffi, Luca Alfonso, Andrea Bersani, Luca Bottura, Stefania Farinon, Francesco Mariani, Samuele Mariotto, Riccardo Musenich, Daniel Novelli, Alessandra Pampaloni, and Tiina Salmi, On behalf of IMCC

***Abstract*—The Muon Collider represents an exciting proposal for a post-LHC accelerator, capable of exploring higher-energy regions with greater power consumption efficiency compared to hadronic alternatives, while avoiding synchrotron radiation limitations inherent in electron colliders. This contribution will focus on the magnets for the Muon Collider storage ring. These magnets pose an unprecedented technological challenge: high magnetic fields are required to ensure the compactness of the ring, maximizing the number of muon beam passes through the interaction region and thereby increasing luminosity. Additionally, large apertures are essential to accommodate an adequate shielding system that keeps the thermal and nuclear loads induced by the beam within acceptable limits. Furthermore, minimizing straight sections is critical to avoid the radioactive hazard posed by collimated neutrino beams, necessitating the use of combined-function magnets (dipole + quadrupole and dipole + sextupole). The interaction region also presents extreme conditions that demand the development of magnets beyond the current state of the art. In this contribution, we will discuss the progress in the feasibility study of magnets for both the arc and the interaction region of the Muon Collider storage ring. Performance limits will be analyzed for dipoles and quadrupoles, taking into consideration constraints on mechanical stresses, margin on the load line, ease of the protection system and cost for ReBCO-based magnets. Finally, the most up-to-date conceptual designs of the arc dipole will be presented, comparing the strengths and challenges of the cos-theta and block coil layouts in terms of achieving of electromagnetic requirements, mechanical structure feasibility, and windability.**

***Index Terms*—Muon collider, superconducting magnets, accelerator magnets.**

I. Introduction

THE Muon Collider is an exciting candidate for a post-LHC facility, offering a unique combination of advantages. Unlike protons, muons are fundamental particles, and compared to electrons, they have a higher mass and emit significantly less synchrotron radiation. These properties enable a muon collider to deliver both high-energy collisions, similar to hadron colliders, and high-precision measurements, typical of electron colliders.

However, the major challenge stems from the muon's short lifetime, approximately 2 μs at rest. This constraint demands extremely rapid production, cooling, acceleration, and collision of muons. Moreover, their decay products must be effectively shielded, and straight sections in the collider ring must be minimized to avoid collimated neutrino fluxes.

To address these technical challenges, the international Muon Collider Collaboration (IMCC), led by CERN [1], has been established and is conducting a feasibility study for such a machine. The current baseline design envisions a 10 TeV center-of-mass collider within a 10 km ring (see Fig. 1).

Due to the limited lifetime of muons, all magnet systems—particularly those in the collider ring [2]—must operate at the frontier of technological capabilities. To ensure compactness and maximize the number of revolutions before decay, the ring magnets must deliver the highest possible magnetic fields. In the interaction regions, quadrupoles must achieve extremely high gradients to reduce β^* and beam emittance, while also providing large apertures to accommodate shielding for decay heat. Combined-function magnets such as dipole-quadrupole and dipole-sextupole are necessary to avoid straight sections that could otherwise lead to dangerous neutrino radiation. In this paper, we present a feasibility study of such magnets, with a focus on REBCO-based HTS magnets, capable of ensuring outstanding electromagnetic performance while promoting sustainability and energy efficiency.

II. Magnets Requirements and Performance Limits

Defining the collider ring magnet requirements demands coordinated input from several Work Packages (WPs), including Cryogenics, Energy Deposition, and Beam Dynamics, in addition to the Magnet WP itself. The Cryogenics WP sets an upper limit on the heat load from muon decay products, which depends on the operating temperature: $5\,\mathrm{W/m}$ for temperatures up to $10\,\mathrm{K}$, increasing to $10\,\mathrm{W/m}$ for higher temperatures. Thanks to studies from the Energy Deposition WP, these heat load constraints have been translated into tungsten shield thickness requirements: 4 cm to respect the $5\,\mathrm{W/m}$ limit, or 3 cm for the $10\,\mathrm{W/m}$ limit [3] [4].

The Beam Dynamics WP has defined the minimum beam pipe diameter, equal to 40 mm (already including the beam screen,

Received 28 July 2025; revised 6 October 2025; accepted 20 October 2025. Date of publication 10 November 2025; date of current version 17 November 2025. This work was supported by European Union under Grant Agreement number 101094300. *(Corresponding author: Barbara Caiffi.)*

Barbara Caiffi, Luca Alfonso, Andrea Bersani, Stefania Farinon, Riccardo Musenich, and Alessandra Pampaloni are with INFN- Genova, 16146 Genova, Italy (e-mail: barbara.caiffi@ge.infn.it).

Luca Bottura is with the European Organization for Nuclear Research (CERN), 1211 Geneva, Switzerland.

Francesco Mariani and Daniel Novelli are with the Sapienza University of Rome, 00185 Rome, Italy, and also with INFN- Genova, 16146 Genoa, Italy (e-mail: daniel.novelli@ge.infn.it).

Samuele Mariotto is with the University of Milan, 20122 Milan, Italy, and also with INFN-LASA, 20090 Milan, Italy.

Tiina Salmi is with Tampere University, 33720 Tampere, Finland.

Color versions of one or more figures in this article are available at https://doi.org/10.1109/TASC.2025.3628590.

Digital Object Identifier 10.1109/TASC.2025.3628590

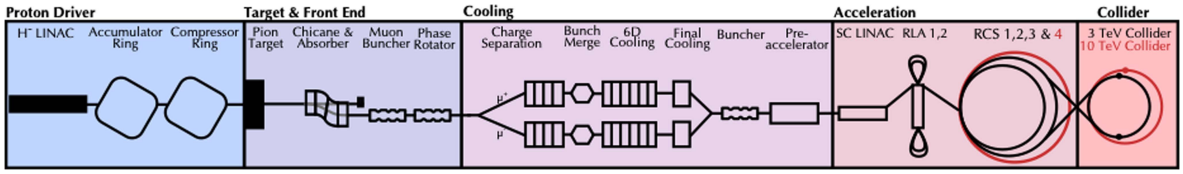

Fig. 1. Muon collider complex.

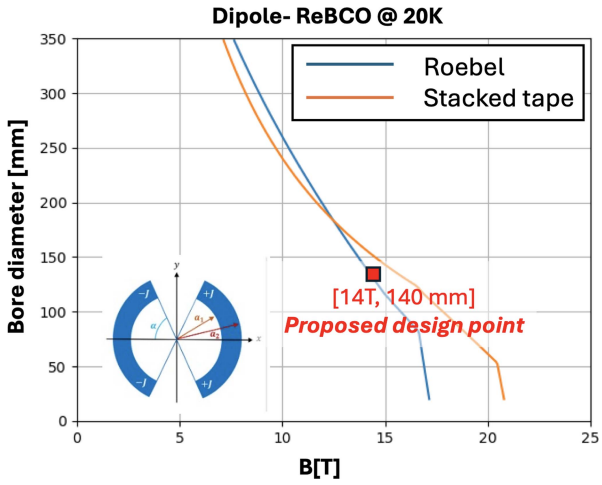

Fig. 2. Upper limits for the ReBCO based dipoles at 20 K with a maximum budget of 400 kEUR/m assuming two different cables: Roebel and stacked tapes, respectively with a superconductor fraction of 0.011 and 0.018.

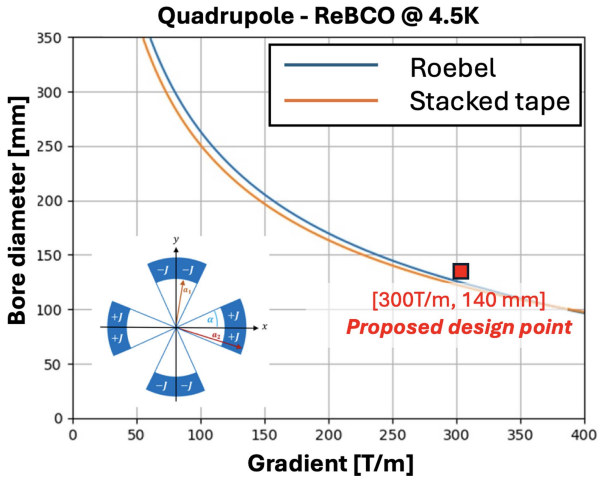

Fig. 3. Upper limits for the ReBCO based quadrupoles at 4.5 K with a maximum budget of 800 kEUR/m assuming two different cables: Roebel and stacked tapes, respectively with a superconductor fraction of 0.011 and 0.018.

the insulation, the heat intercept and the clearance), which determines the magnet aperture range from 140 to 160 mm, depending on the operating temperature. Specifically, using HTS materials allows operation at 20 K with a 3 cm tungsten shield and a 140 mm magnet aperture. Conversely, with LTS technology, respecting the $5\,\mathrm{W/m}$ limit requires a 4 cm shield, resulting in a 160 mm aperture. In both cases, we refer to an aperture approximately three times larger than that of typical accelerator magnets. As shown in Fig. 4, the LHC Main Bending Dipole easily fits within the bore of our arc dipoles. To guide

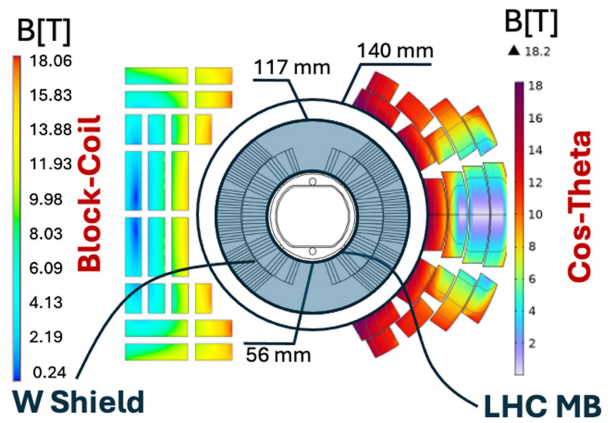

Fig. 4. Block (on the left) and cosθ (on the right) coil cross-sections of the two proposed layouts. LHC Main Bending Dipole is also shown as a reference for scale.

magnet design and provide a quick feedback to the Beam Dynamics WP on the preliminary versions of the lattice designs, a novel approach has been implemented combining analytical estimates with finite element (FEM) simulations [5][6]. This method evaluates upper limit curves in the field–aperture plane for dipoles and in the gradient–aperture plane for quadrupoles, while incorporating key constraints:

- *Load-line margin:* Set to 2 K for NbTi at 1.9 K (LHC-based), 2.5 K for Nb_3 Sn at 4.5K (Hi-Lumi LHC target), and 2.5 K for REBCO at 20 K, the latter based on cryogenic system stability rather than critical surface limits.
- *Mechanical stress:* Maximum allowable compressive stress is 100 MPa for NbTi, 150 MPa for Nb $_3$ Sn, and 400 MPa for REBCO, derived from material datasheets and literature [7].
- *Protection feasibility:* Hotspot temperature limits are 250 K for NbTi and Nb $_3$ Sn, and 200 K for REBCO. A delay time of 40 ms is assumed for insulated conductors, and 1 ms for metal-insulated REBCO. [8]

These constraints define the feasible parameter space for different technologies and operating conditions, such as temperature and cost, set as free parameters that can vary to perform sensitivity studies. Following this approach, A-B plots were generated for Nb-Ti, Nb_3 Sn, and ReBCO, considering different budget ranges (from 120 kEur/m to € 800 kEur/m) and operating temperatures between 4.5K and 20K, as reported in previous works [2], [5], [6]. From these preliminary studies,REBCO-based magnets emerged as the only credible option capable of meeting all requirements while ensuring an energy-efficient and sustainable machine. For this reason,they are the sole focus of discussion in this paper.

Fig. 2 shows the upper performance limits of ReBCO-based dipoles at an operating temperature of $T_{\mathrm{op}} = 20\,\mathrm{K}$ and under a

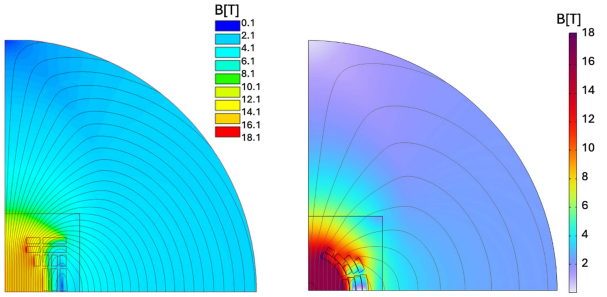

Fig. 5. Magnetic field map across one quarter of the magnet cross section for the two studied layouts (block coil on the left, cosθ coil on the right), including the coil and the iron yoke.

TABLE I
MAIN PARAMETERS FOR BLOCK AND COSθ COIL LAYOUTS

Parameter	Block coil	Cosθ coil
I_{OP} [A]	3515	3700
J_{ENG} [A/mm^2]	542	571
J_{COPPER} [A/mm^2]	1820	1916
B_1 [T]	16	16
B_{PEAK} [T]	18.1	18.2
T_{OP} [K]	20	20
$\Delta T_{\mathrm{MARGIN}}$ [K]	$2.5 \pm 1\%$	$2.5 \pm 1\%$
Aperture [mm]	140	140
$E_{\mathrm{STORED}}/$ [J/mm^3]	0.3	0.29
E_{STORED}/L [MJ/m]	5.3	3.9
L [mH/m]	853	534
N_{tapes}	10720	8272

maximum cost constraint of 400 kEUR/m, which correspond to the current baseline parameters for the collider arcs. The magnet cost per unit length is estimated according to the model described in Section IV. Two cable layouts are considered: Roebel and stacked tapes, with respective superconductor filling factors of 0.011 and 0.018. The stacked tape configuration has been adopted as the baseline for the conceptual design study, as further discussed in Section III.

Fig. 3 presents the upper performance limits for ReBCO-based quadrupoles, using the same two cable types. In this case, the baseline temperature and cost are set to 4.5 K and 800 kEUR/m, which reflect the more demanding requirements of the IR. Based on these results, two candidate working points are identified: a 14 T dipole for the arc and a 300 T/m quadrupole for the IR, both with a 140 mm aperture. These working points have been proposed as milestone technology demonstrators in the supplementary report to the European Strategy for Particle Physics [9]. The goal is to complete their construction by 2045, with an estimated investment of 15.8 MCHF and 126 FTEy for the dipole, and 8.8 MCHF and 60 FTEy for the quadrupole, respectively.

III. ARC DIPOLE CONCEPTUAL DESIGNS

While analytical tools provide valuable guidance during the design phase, they must be complemented by detailed engineering models. The conceptual designs currently under development feature arc dipoles with both block and cosθ coil layouts, as illustrated in Fig. 4, and incorporate several improvements over previous publications [2], [11], [12].

The cable configuration remains unchanged: REBCO conductors are arranged in a stacked layout composed of two 12 mm-wide tapes (Fujikura FESC type with artificial pinning centers, used as a reference for both geometry and electrical performance), co-wound with a 50 μm thick stainless steel strip serving as metallic insulation, as detailed in earlier work.

Twisted conductor geometries such as CORC and Roebel cables were excluded from consideration due to their complexity and the limited benefits they offer in terms of AC loss reduction [13].

Fig. 4 shows the status of the art of the coil cross-sections of the two proposed layouts side by side for comparison, along with the LHC Main Bending Dipole to provide a size reference. Additionally, the magnetic field distribution is illustrated using a color scale, as in Fig. 5 where one quarter of the overall magnets including the coil and the iron yoke is shown.

The block coil concept achieves a 16 T central field and an 18.1 T peak field. It features 7 vertically stacked blocks resembling cosθ geometry but without keystoning, easing winding around the bore. 4 upper blocks use a racetrack layout, avoiding bending being located above the beam pipe aperture. This design promises better manufacturability and easier stress management, pending winding validation.

The cosθ layout achieves similar fields (16.1 T bore, 18.2 T peak), and allows for reduced conductor volume (25% less) and easier field quality optimization. However, it poses greater challenges for mechanical stress management. It consists of four layers, containing respectively 3, 4, 2 and 2 blocks. Unlike in the block coil case, the non-uniform current distribution resulting from screening currents is already taken into account, using both an analytical MATLAB-based model following Brandt's approach [10] and the T-A formulation, a numerical method implemented in COMSOL. While the latter is computationally more demanding, it enables the inclusion of nonlinear effects such as the magnetization of the iron yoke and the time-dependent hysteretic behavior of persistent currents within the REBCO tapes.

The main parameters of the two models are listed in Table I and more details about can be found in the dedicated papers [14] and [15], where also the hysteretic losses and the quench aspects are analyzed.

A preliminary mechanical analysis has also been conducted for both concepts, focusing on the stress induced by Lorentz forces on the coils. The coils were modeled as homogeneous blocks with a Young's modulus of 174 GPa and Poisson's ratio of 0.3 [16], encapsulated within an infinitely rigid support structure.

Assembly and cooldown effects are not yet considered in this analysis, and the mechanical structure itself still requires a more realistic description, which will be developed in the next phase of the study.

The principal stress distribution for the block coil configuration, along x and y directions, is shown in Fig. 6, and is compared with a previous layout version published in [11]. A stress-management strategy has been implemented: coil blocks, which were previously monolithic, have been subdivided into smaller sections separated by mechanical spacers designed to partially intercept Lorentz forces and redistribute them more effectively. As a result, the peak stress along the x -direction is reduced from -238 MPa to -216 MPa, and along the y -direction from -218 MPa to about -60 MPa.

A more refined analysis, incorporating realistic mechanical properties for the spacers, is currently underway.

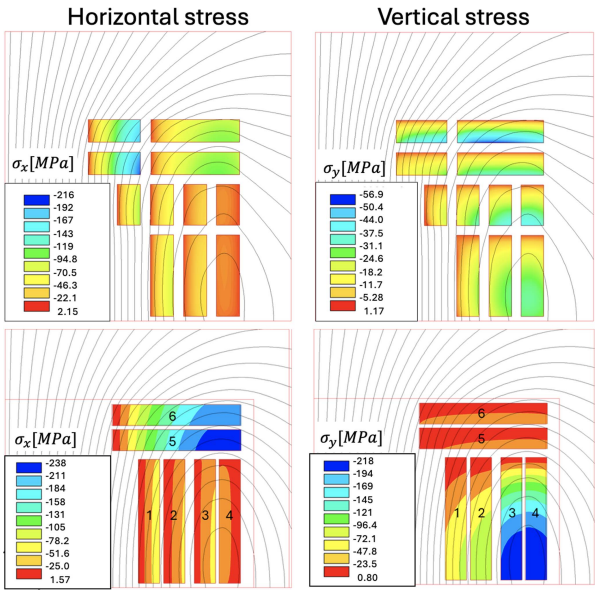

Fig. 6. Stress map showing the distribution of mechanical stress along the x-direction (horizontal) and y-direction (vertical) induced solely by Lorentz forces for the block coil layout. For completeness, the previous design from [11] is also included (botton left and right), to illustrate the impact of the applied stress-management strategy.

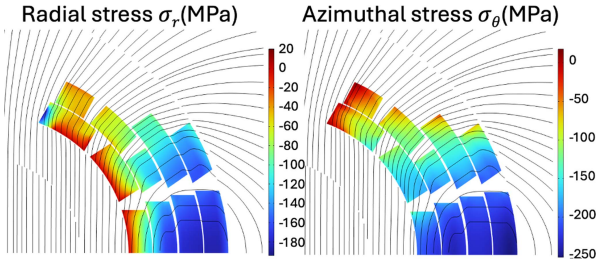

Fig. 7. Stress map showing the distribution of mechanical stress along the radial and the azimuthal direction induced solely by Lorentz forces for the cosθ layout.

TABLE II
COMPARISON OF MAXIMUM STRESS COMPONENTS FOR BLOCK COIL AND COSθ COIL LAYOUTS

Parameter	Block coil	Parameter	Cosθ coil
$\sigma_{X,\mathrm{MAX}}$ [MPa]	-216	$\sigma_{r,\mathrm{MAX}}$ [MPa]	-194
$\sigma_{Y,\mathrm{MAX}}$ [MPa]	-56.9	$\sigma_{\theta,\mathrm{MAX}}$ [MPa]	-252

Fig. 7 shows the principal stresses in the r and θ directions for the cosθ configuration. In this case, no stress-management strategy has been applied yet, and the stress along the radial direction exceeds the allowable limit of 100MPa for the compressive stress on the thinner tape side [16].

The maximum stress in the principale directions for the two models are listed in Table II.

IV. COST MODEL

The cost model used in this work has been revised and improved with respect to previous studies already cited. The estimated cost per unit length of the magnet is given by $\frac{C}{L} = C_{\mathrm{coil}} + C_{\mathrm{ColdMass}} + C_{\mathrm{CryoMagnet}}$.

TABLE III
COST AND MATERIAL PARAMETERS FOR THE REBCO-BASED MAGNET

	REBCO (aspirational)	Unit
c_{Strand}	2671	EUR/kg
d_{Strand}	7800	kg/m^3
f_{Cable}	0.0	(-)
$C_{\mathrm{CoilManufacturing}}$	9.9	kEUR/m
$C_{\mathrm{ColdMassMaterialsRef}}$	25	kEUR/m
B_{Ref}	8.33	T
$C_{\mathrm{ColdMassManufacturing}}$	26.4	kEUR/m
$C_{\mathrm{CryoMagnet}}$	8.0	kEUR/m

TABLE IV
ESTIMATED MAGNET COST PER UNIT LENGTH

	C_{coil} [kEUR/m]	C_{ColdMass} [kEUR/m]	C_{Cryostat} [kEUR/m]	C_{tot} [kEUR/m]
Block coil	303	74	8	385
Cosθ coil	236	74	8	318

The coil cost includes three contributions, $C_{\mathrm{coil}} = C_{\mathrm{SC}} + C_{\mathrm{Cable}} + C_{\mathrm{CoilManufacturing}}$. The first term accounts for the superconducting material itself. The second term refers to cabling and insulation, and is estimated as a fraction f_{Cable} of the superconductor cost, $C_{\mathrm{Cable}} = f_{\mathrm{Cable}} \cdot C_{\mathrm{SC}}$ The third term represents the cost of coil manufacturing. The cold mass cost is composed of material and manufacturing contributions. The material cost scales with the magnetic field intensity, under the assumption that higher B values require more iron for magnetic return and result in stronger Lorentz forces, increasing the complexity of the support structure. This contribution is scaled with respect to a reference case as $C_{\mathrm{ColdMassMaterials}} = \frac{B}{B_{\mathrm{ref}}} \cdot (C_{\mathrm{ColdMassMaterials}})_{\mathrm{ref}}$.

The cost model parameters adopted in this analysis are summarized in Table III. An aspirational unit cost of 2671 EUR/kg is assumed for the REBCO material, approximately one third of the current market price (8000 EUR/kg). The remaining parameters are based on experience from Hi-Lumi and LHC projects. Since a no-insulation REBCO cable is considered, the cabling factor f_{Cable} is set to zero.

Using this model and the reference values listed above, the estimated cost per unit length of the arc dipole was computed for both the cosθ and block coil configurations, as shown in Table IV. The conductor cost for the cosθ layout is about 25% lower, consistent with the reduced amount of cable required.

V. CONCLUSIONS AND OUTLOOK

The feasibility study for a 10 TeV Muon Collider is ongoing within the IMCC. Magnet design requirements are being defined in coordination with beam dynamics, energy deposition, and cryogenics working groups, using upper performance limits derived from an innovative analysis of stress, margin, and protection feasibility. Conceptual designs for cosθ and block coil dipoles are in progress, including electromagnetic and mechanical modeling. The development of HTS demonstrators is a critical milestone to validate these design approaches, as emphasized in the European Strategy for Particle Physics.

ACKNOWLEDGMENT

The authors thank all members of the IMCC Working Groups.

REFERENCES

[1] C. Accettura et al., "Towards a Muon Collider," *Eur. Phys. J. C*, vol. 83, no. 9, 2023, Art. no. 864, doi: 10.1140/epjc/s10052-023-11889-x.

[2] B. Caiffi et al., "Challenges and perspectives of the superconducting magnets for the Muon Collider storage ring," *IEEE Trans. Appl. Supercond.*, vol. 35, no. 5, Aug. 2025, Art. no. 4002007, doi: 10.1109/TASC.2025.3529424.

[3] P. B. D. Sousa et al., "Muon Collider magnet technology options internal review–cooling," in *Proc. IMCC Annu. Collaboration Meeting*, CERN, Geneva, Switzerland, 2023, pp. 19–22. [Online]. Available: https://indico.cern.ch/event/1250075

[4] A. Lechner et al., "Radiation shielding studies for superconducting magnets in multi-TeV muon colliders," *JACoW Publishing*, doi: 10.18429/JACOW-IPAC2024-WEPR26, pp. 2536–2539, 15.

[5] D. Novelli et al., "Analytical evaluation of dipole performance limits for a Muon Collider," *IEEE Trans. Appl. Supercond.*, vol. 34, no. 5, 2024, Art. no. 4002405, doi: 10.1109/TASC.2024.3352526.

[6] D. Novelli et al., "Analytical and numerical study of superconducting dipole and quadrupole performance limits for a Muon Collider," *IEEE Trans. Appl. Supercond.*, vol. 35, no. 5, 2025, Art. no. 4000205, doi: 10.1109/TASC.2024.3507744.

[7] Fujikura, "HTS tape online catalogue," 2025. [Online]. Available: https://www.fujikura.co.jp/products/superconductors/images/Fujikura_superconductor_EN.pdf

[8] T. Salmi et al., "Analytical estimation of quench protection limits in insulated, non-insulated, and metal-insulated ReBCO accelerator dipoles and quadrupoles," *IEEE Trans. Appl. Supercond.*, vol. 35, no. 5, Aug. 2025, Art. no. 4604705, doi: 10.1109/TASC.2025.3540791.

[9] L. Bottura et al., "Magnet R&D for the Muon Collider–european strategy input," 2025, *arXiv:2503.21185*.

[10] E. H. Brandt and M. Indenbom, "Type-II-superconductor strip with current in a perpendicular magnetic field," *Phys. Rev. B*, vol. 48, no. 17, 1993, Art. no. 12893.

[11] L. Alfonso et al., "Preliminary design of a block-coil magnet for the Muon Collider ring," *IEEE Trans. Appl. Supercond.*, vol. 35, no. 5, Aug. 2025, Art. no. 4000405, doi: 10.1109/TASC.2024.3510234.

[12] F. Mariani et al., "Preliminary electromagnetic and mechanical design of a COS dipole for the Muon Collider study," *IEEE Trans. Appl. Supercond.*, vol. 35, no. 5, Aug. 2025, Art. no. 4000805, doi: 10.1109/TASC.2024.3519077.

[13] D. Uglietti et al., "Non-twisted stacks of coated conductors for magnets: Analysis of inductance and AC losses," *Cryogenics*, vol. 110, 2020, Art. no. 103118, doi: 10.1016/j.cryogenics.2020.103118.

[14] L. Alfonso et al., "Update on the preliminary electromagnetic and mechanical design of the block-coil dipole for the muon collider ring," *IEEE Trans. Appl. Supercond.*, vol. 35, no. 5, Aug. 2025, Art. no. 4000405.

[15] F. Mariani et al., "Conceptual electromagnetic and mechanical design of a Cosθ dipole for the Muon Collider study," *IEEE Trans. Appl. Supercond.*, vol. 35, no. 5, Aug. 2025, Art. no. 4000805.

[16] C. Barth et al., "Electro-mechanical properties of REBCO coated conductors from various industrial manufacturers at 77 k., self-field and 4.2 k., 19 t," *Supercond. Sci. Technol.*, vol. 28, 2015, Art. no. 045011.

[17] "IMCC supplementary report to the European strategy, *arXiv:2504.21417*.